Progress In Electromagnetics Research C, Vol. 136, 151–160, 2023

Four Element MIMO Antenna for Wireless Body Area Network and Advanced Wireless Services Applications

Nelapati Ananda Rao[1, *] and Lalitha B. Konkyana[2]

Abstract—A Multi-Input Multi-Output (MIMO) dual-band antenna useful for advanced wireless services (AWSs) and wireless body area network (WBAN) applications is presented. To have dual bands of operation two techniques were used namely, Defective Ground Structure (DGS) and slotted patch. The lower operating band is spread over 108 MHz from 2.106 GHz to 2.214 GHz which covers AWS, UMTS, and LTE bands. The upper operating band is spread over 221 MHz from 4.141 GHz to 4.362 GHz which covers the WBAN band. The lower operating band is the result of perforation in the patch and inverted T-shaped ground, and the upper operating band is due to the two rectangular slots placed diagonal to each other in the patch and perforations in the ground. High isolation among MIMO elements is observed through a low Envelope Correlation Coefficient (ECC) of 0.0004. The design of a 2×2 MIMO antenna is realized using FR4 material with a size of $70\,\text{mm} \times 70\,\text{mm} \times 1.524\,\text{mm}$ and Ansys HFSS tool. A high level of correlation between simulated and experimental results is observed which enables the presented MIMO antenna to be perfect for the proposed AWS and WBAN applications.

1. INTRODUCTION

Nowadays healthcare systems are developed to a level that they can predict health complications by continuously monitoring human vitals, and we also have many systems which enable doctors to track and observe patients' health conditions from remote locations. All these are possible because of communication devices which are compact and implanted in the human body or on the surface of the body or in the clothes, etc. These devices collect information from the biomedical sensors which can measure the biological signals and transmit them via these communication devices. These types of systems are called WBAN, and they use AWS like Universal Mobile Telecommunications System (UMTS) and Long Term Evolution (LTE) for communication.

Many MIMO antennas were developed by researchers to meet these requirements. In [1], a dual wideband antenna with dual polarizations is proposed which covers the frequencies of 3.24 GHz to 4.07 GHz and 4.28 GHz to 5.23 GHz. The antenna has a size of 137.6 mm × 102.6 mm, which is comparatively large, and circular polarization, which will lead to the reduction of the power level by 3 dB and in turn affects the data transmission. In [2], a MIMO antenna with high isolation was proposed for smartwatches. It has an operating frequency band covering 2.4 GHz to 2.49 GHz. Here high isolation is achieved by employing the technique of having two degenerative modes in the design of the MIMO antenna. But having a degenerative mode of operation is not viable for our applications of WBAN and AWS. In [3], a self-isolated MIMO antenna is presented in which a substrate integrated waveguide technique is implemented to achieve self-isolation. The operating range is 3.47 GHz to 3.53 GHz. Here dual feeds are used for a single radiating element, and isolation improvement is shown among the two feeds which do not apply to normal MIMO antennas where different radiating elements will have different feeds. In [4], a single layer triple polarized antenna is presented working in the sub-6 GHz band, and here

Received 20 May 2023, Accepted 19 July 2023, Scheduled 17 August 2023

* Corresponding author: Nelapati Ananda Rao (nar_ece@vignan.ac.in).

[1] Vignan's Foundation for Science Technology and Research, Andhra Pradesh, India. [2] Aditya Institute of Technology and Management, Andhra Pradesh, India.

the antenna has triple feeds making the antenna MIMO. Different individual inputs and combinations of inputs enable diversified operating modes in the antenna, which are generated by a large number of vias that are introduced in the antenna. In [5], mutual coupling is reduced using an Electromagnetic Band Gap (EBG). Here the antenna radiates at the frequency of 6 GHz. The EBG structure used is a spiral structure which is made as an array of elements placed in between the two antenna elements. Here though isolation is enhanced it also requires additional structures to be incorporated in the antenna array for reduction of coupling. [6] uses a DGS to design a multiband antenna. A single frequency 2×2 antenna array has been designed, and DGS is introduced to generate resonance at multiple frequencies. Introducing a DGS also helped in attaining good impedance matching. All frequencies obtained were between 5 and 8 GHz and are thus commonly used in C-band applications. [7] proposes a fractal DGS for miniaturization. Bandwidth comparison is presented for antennas with and without DGS. Operating frequency shifts to 1.2 GHz from 2.56 GHz and 1.657 GHz from 3.72 GHz, respectively. With the implementation of DGS, antenna bandwidth is increased by 72%, and the size is reduced.

Similarly, many antennae [8–25] were developed with different techniques to increase the isolation, decrease the mutual coupling, or enhance the parameters like ECC, but all of these antennas have a limitation in terms of throughput and ECC which is necessary for the proposed applications of AWS and WBAN. Here we propose a MIMO antenna with low coupling and ECC without any additional structure in the antennas with dual frequencies of operation.

2. EVOLUTION OF PROPOSED ANTENNA

The proposed MIMO antenna of 2×2 elements which are placed orthogonally to one another helps in the reduction of coupling and ECC among the antenna elements. Figure 1 depicts the evolution of the

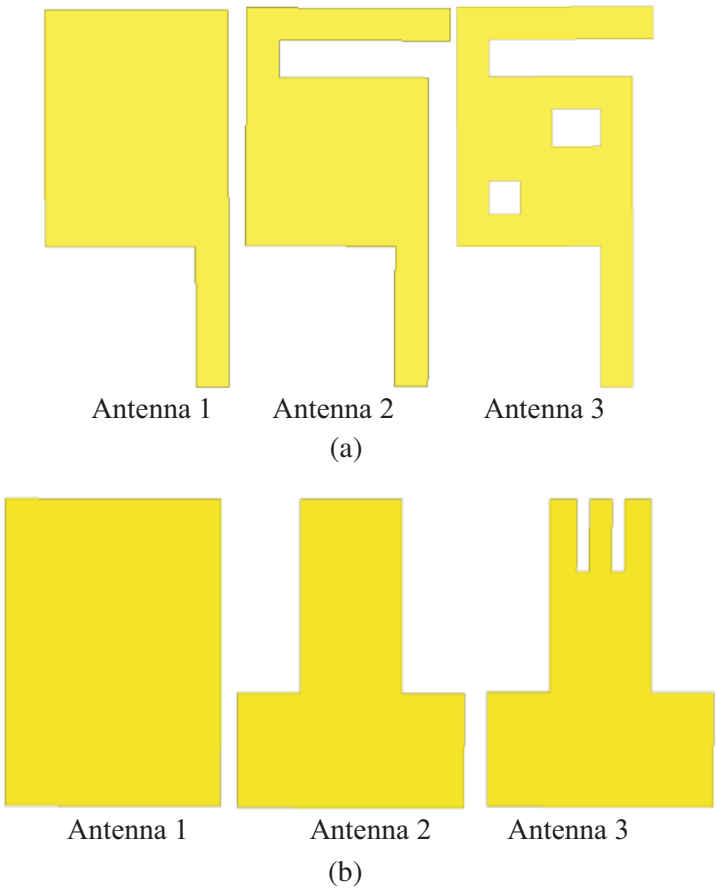

Figure 1. Antenna evolution stages. (a) Radiating element. (b) Ground plane.

antenna in stages. Antenna 1 has a basic radiating element as a rectangle and is excited with a 50 Ω strip line feed with a uniform ground plane. In antenna 2, the patch is perforated with a rectangle of size 15.5 mm × 3 mm, and the uniform ground is replaced with an inverted T-shaped ground. In antenna 3, the patch is further etched with a pair of diagonal slots of dimensions 4.6 mm × 3.4mm and 3 mm × 3 mm, and the ground is perforated twice with rectangles of size 7.4 mm × 1.5 mm.

The MIMO antenna was designed with four elements which are placed orthogonal to one another. Figure 2 shows the top view and rare view of the simulated and fabricated MIMO antennas, while Table 1 lists the optimum dimensions of the antenna element.

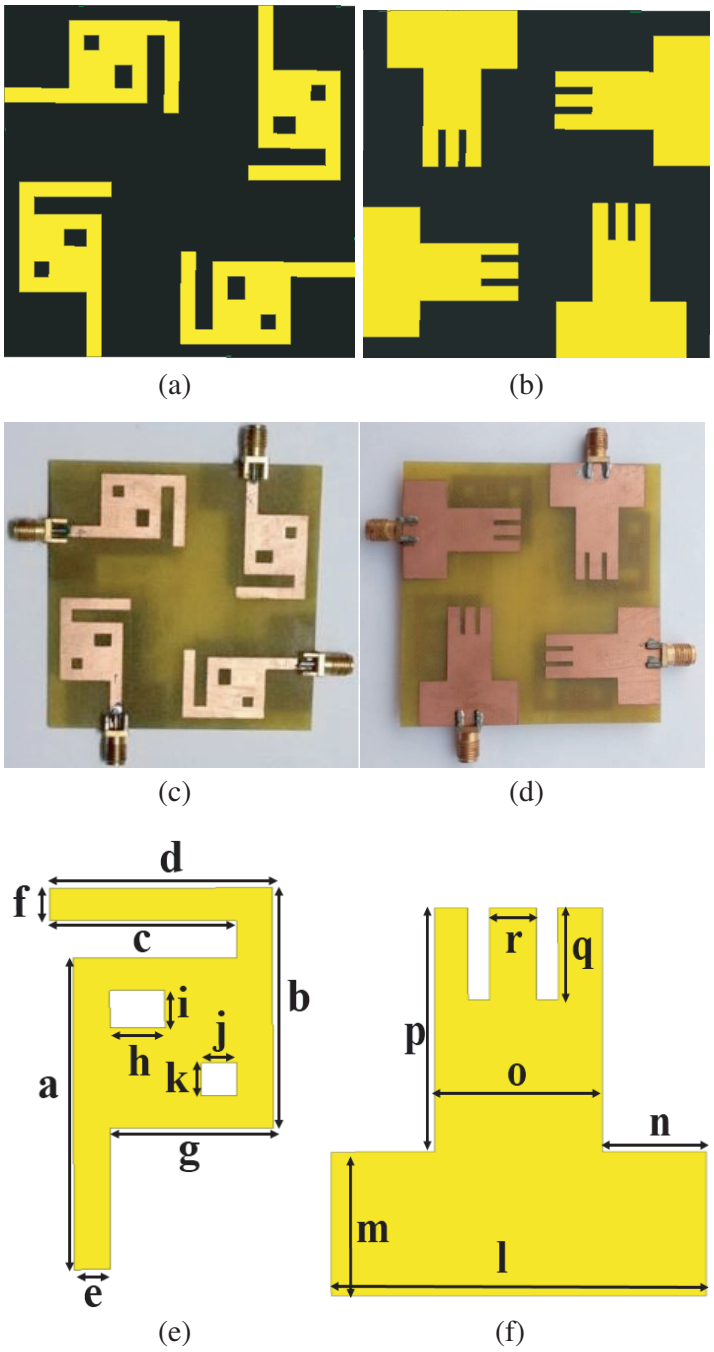

Figure 2. MIMO antenna structure. (a) Top view. (b) Rare view. (c) Top view (Fabricated). (d) Rare view (Fabricated). (e) Radiating element. (f) Defective Ground Structure.

Table 1. Antenna dimensions (Optimized).

Parameter	Value (mm)	Parameter	Value (mm)
a	28.5	j	3
b	22	k	3
c	15.5	l	26
d	18	m	11.7
e	3	n	7
f	3	o	11.6
g	13.45	p	19.7
h	4.6	q	7.4
i	3.4	r	2.5

3. RESULTS AND ANALYSIS

Various antenna parameters that affect the antenna performance were studied and presented. Figure 3 presents the S_{11} at different evolution stages of the antenna and a comparison of simulated and measured S_{11}. Antenna 1 with a uniform plane ground and a rectangular patch has a wideband operating range from 3.5 GHz to 4.5 GHz. But with the introduction of the perforation in the patch and inverted T-shaped ground plane, the wideband of operation is converted to the dual bands of operation at 2.16 GHz and 4.27 GHz. Here we can observe that the impedance of the antenna is not in tune at 4.4 GHz. To enhance it, two square slots of unequal dimensions, which are diagonally placed, are etched in the perforated patch, and a pair of rectangular perforations are made in the inverted T ground plane. With these further slots and perforations, the impedance matching at the higher band is enhanced, and it radiates at 4.27 GHz. Finally, the proposed antenna has dual frequencies of operation. The center frequency at the lower side is at 2.16 GHz, and the upper side is at 4.27 GHz with a 10 dB impedance bandwidth of 108 MHz and 221 MHz, respectively. The lower operating band is spread over 2.106 GHz to 2.214 GHz which covers AWS, UMTS, and LTE bands. The upper operating band is spread over 4.141 GHz to 4.362 GHz which covers the WBAN band.

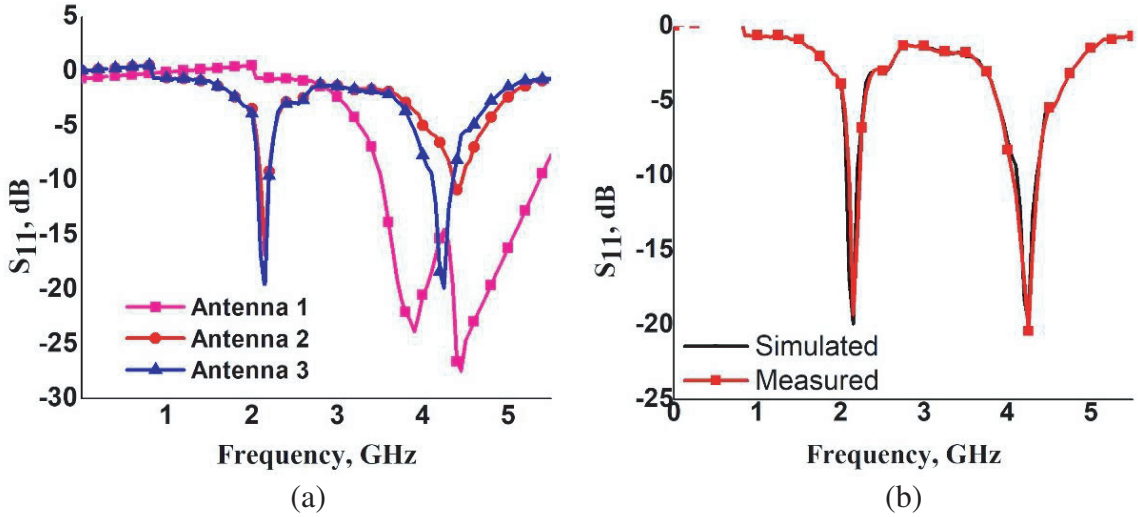

Figure 3. Return loss. (a) S_{11} of the proposed antenna in different stages. (b) S_{11} comparison of simulation and measured antenna.

The proposed antenna is intended for the AWS and WBAN applications, which require a system that can communicate with multiple sensors in parallel mode in a small region. So here antennas with moderate gain are necessary for the system to meet the standards of Specific Absorption Rate (SAR). The gains of 3.47 dB at the lower band of 2.16 GHz and 3.49 dB at the higher band of 4.27 GHz are presented in Figure 4.

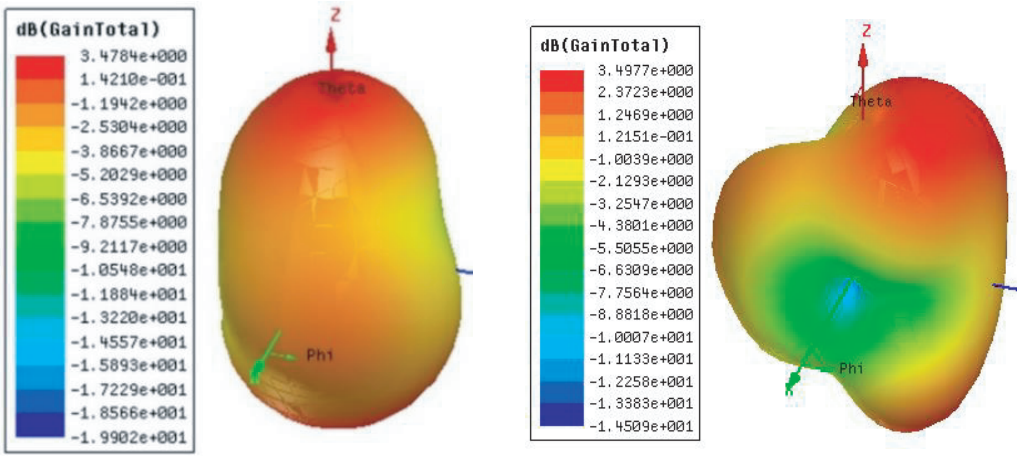

(a) (b)

Figure 4. Gain of the proposed antenna. (a) At 2.16 GHz. (b) At 4.27 GHz.

Mutual coupling is the major drawback in any MIMO antenna and is measured by ECC, and a MIMO antenna should have very low mutual coupling and ECC for efficient transmission of data and to achieve high throughput. Here we have addressed these two design problems with a simple solution by placing antennas in an orthogonal manner in the MIMO structure. By placing antennas in an orthogonal manner, the radiating fields of the antennas are also orthogonal to each other which will reduce the phase Cancellation of the signals in both near fields and far-field which will improve the isolation among antenna elements and reduce ECC which is shown in Figures 5 and 6.

The radiation plots (simulated and measured) at the two operating frequencies are presented in Figure 7.

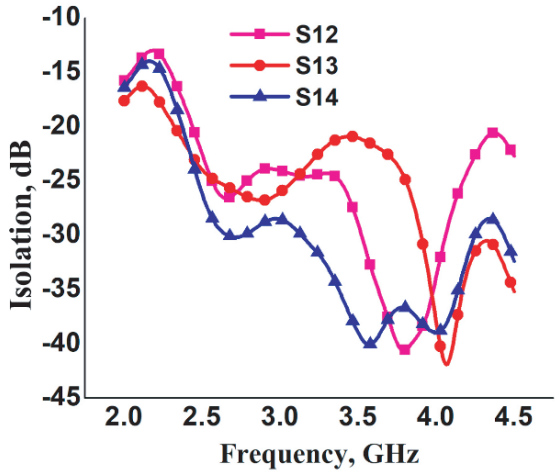

Figure 5. Mutual coupling among MIMO antenna elements.

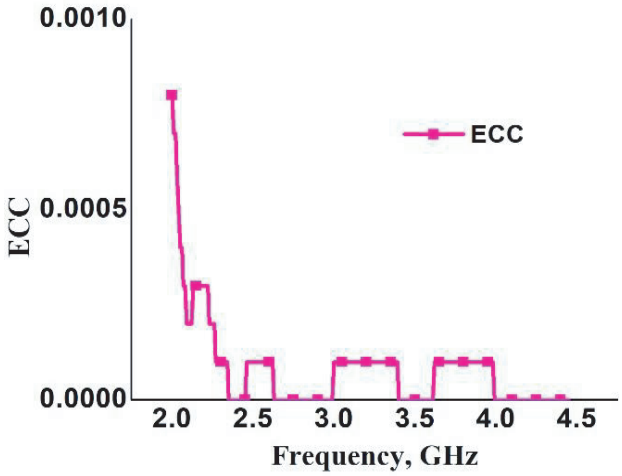

Figure 6. Envelope correlation coefficient.

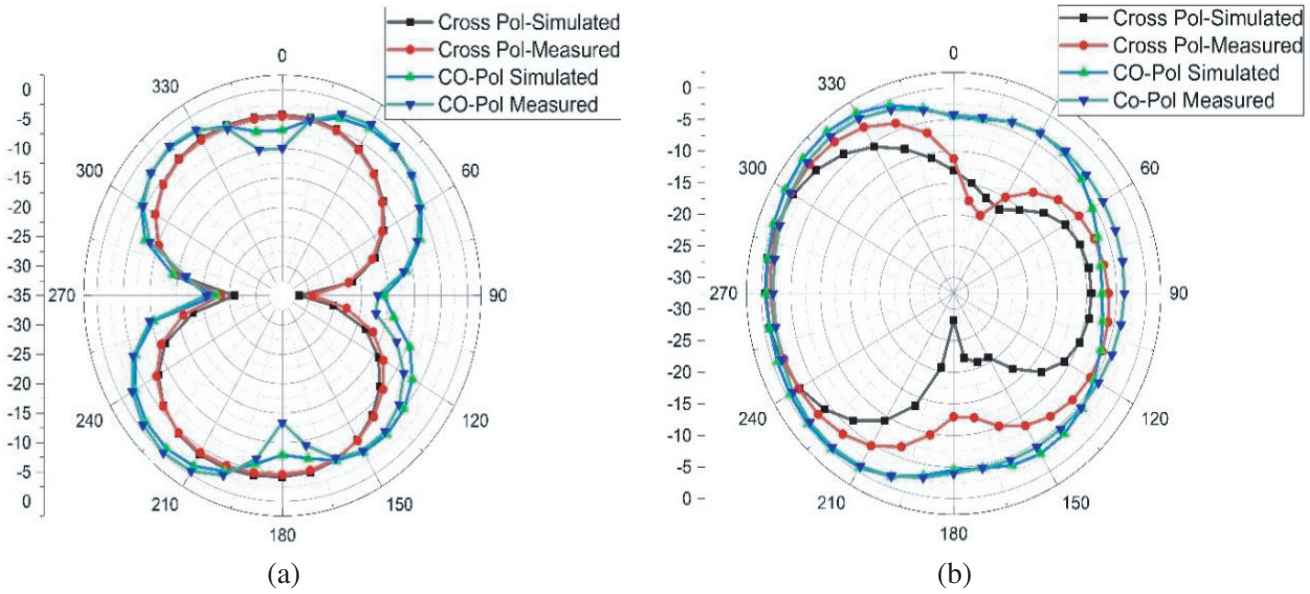

Figure 7. Radiation patterns. (a) At 2.16 GHz. (b) At 4.27 GHz.

At the lower band, we can observe that the Co-Polarization and Cross-Polarization plots have an 8-shaped pattern with uniform distribution of radiation in the cross-pole. But at the Co-Polarization, we can observe a small dip at 0° and 180° which may be due to the slots in the patch and the nonuniform current distribution in the patch due to these diagonal slots. Similarly, at a higher operating band, we can observe that the simulated and measured Co-Polarization and Cross-Polarization plots have an omnidirectional pattern with uniform distribution of radiation in the Co-Polarization. But at the cross-pole, we can observe a reduction in the power of the antenna on half side of the pattern which may be due to the rectangular perforation in the patch and the nonuniform current distribution in the patch due to the perforation.

The proposed antenna is intended for AWS and WBAN applications, which require a system that can communicate with multiple sensors in parallel mode in a small region. So here antennas with good directivity are necessary for the system to meet the short communication ranges. The proposed antenna has a directivity of 4.6 dB at the lower band of 2.16 GHz and 4.48 dB at the higher band of 4.27 GHz which are presented in Figure 8.

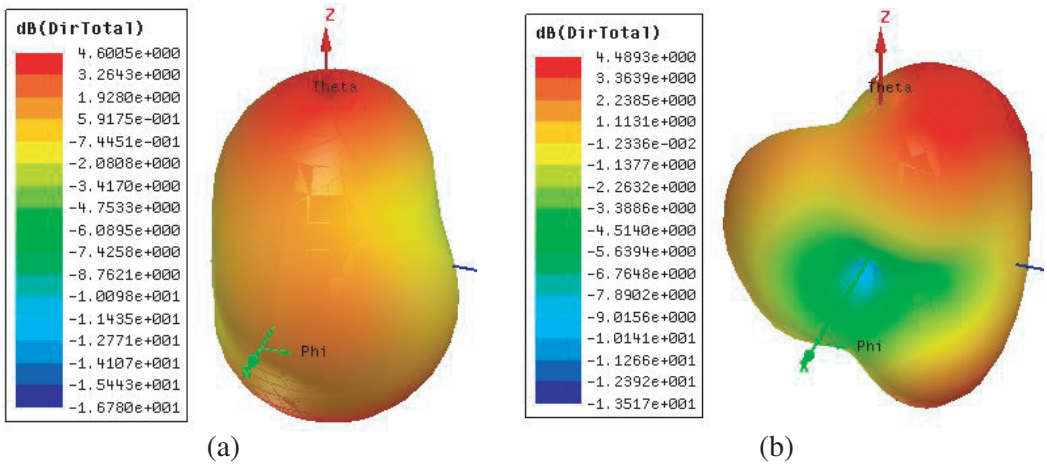

Figure 8. Directivity. (a) At 2.16 GHz. (b) At 4.27 GHz.

Figure 9 shows the current distributions of the antenna at the two operational frequency bands. Figure 9(a) shows the radiating elements at 2.16 GHz. We can observe that the radiation is mainly due to the rectangular perforation and the slot near it. Figure 9(b) depicts the current fields of the ground

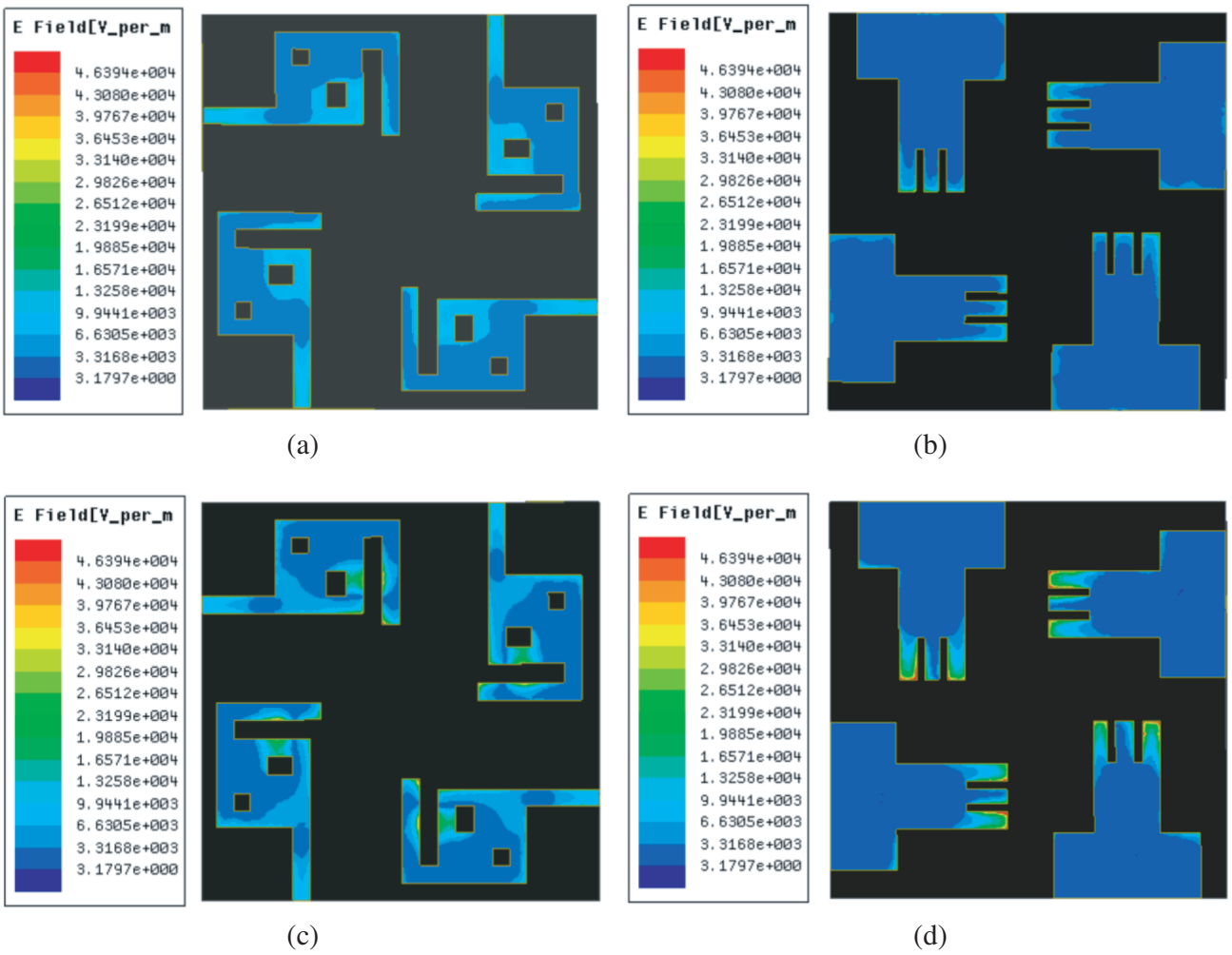

Figure 9. Current field distribution. (a) At 2.16 GHz. (b) At 2.16 GHz. (c) At 4.27 GHz. (d) At 4.27 GHz.

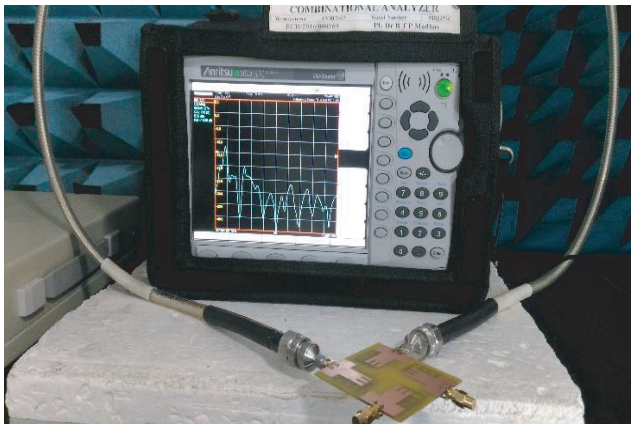

Figure 10. Realized antenna and measurement setup.

plane at 2.16 GHz, and here we can see that the radiation is generated by perforation in the ground plane. Figure 9(c) depicts the current fields of the radiating elements at 4.27 GHz. We can observe that the radiation is mainly due to the rectangular perforation and feed line. Figure 9(d) shows the current distributions of the ground plane at 4.27 GHz, and here we can see that the radiation is due to the T structure in the ground plane.

In Figure 10, we can view the mutual coupling plot of the MIMO antenna in measurement setup utilizing a vector network analyzer.

Table 2 compares the proposed antenna with reported dual band antennas. The proposed antenna performs better in terms of gain and antenna profile.

Table 2. Proposed antenna comparison with reported antennas.

Ref.	Frequency (GHz)	Gain (dB)	Size (λ^2)
[22]	2.5–2.7 3.45–3.8	2.5 2.7	$0.63 * 1.25$
[23]	1.87–2.53 3.6–3.8	3.86 4	$0.37 * 0.62$
[24]	1.8–2.69 3.4–3.6	2.3 3.5	$0.35 * 0.2$
[25]	1.55–2.65 3.35–3.65	2.2 3.8	$0.3 * 0.31$
Proposed Work	2.10–2.21 4.14–4.36	3.47 3.49	$0.24 * 0.24$

4. CONCLUSION

A 2×2 MIMO antenna with two operating frequency bands is presented. Radiating elements have a rectangular perforation and a pair of diagonal slots. A defective ground structure is taken in an inverted T shape with perforations. The perforation in the patch and inverted T-shaped ground generated the lower operating band in the upper band due to the diagonal slots in the patch and perforations in the ground. The lower band is at 2.16 GHz, and the upper band is at 4.27 GHz with a 10 dB impedance bandwidth of 108 MHz and 221 MHz, respectively. Mutual coupling at the lower and higher bands is around -13 dB and -30 dB, respectively, which presents a low coupling effect among the antenna elements. The gain of the individual antenna element is 3.47 dB at 2.16 GHz and 3.49 dB at 4.27 GHz. ECC is one of the crucial parameters in a MIMO antenna which shows the isolation among the antenna elements and also the amount of data rate transmitted from the MIMO antenna. A very low level of ECC, 0.0003, is observed which presents a very high level of isolation in the MIMO antenna. Omnidirectional radiation pattern is observed at both frequencies which is essential for the WAS and WBAN applications.

REFERENCES

1. Feng, B., C. Zhu, J.-C. Cheng, et al., "A dual-wideband dual-polarized magnetoelectric dipole antenna with dual wide beamwidths for 5G MIMO microcell applications," *IEEE Access*, Vol. 7, 43346–43355, April 2019.
2. Wen, D., Y. Hao, H. Wang, and H. Zhou, "Design of a MIMO antenna with high isolation for smartwatch applications using the theory of characteristic modes," *IEEE Transactions on Antennas and Propagation*, Vol. 67, No. 3, March 2019
3. Niu, B.-J. and J.-H. Tan, "Compact self-isolated MIMO antenna system based on quarter-mode SIW cavity," *Electronics Letters*, Vol. 55, No. 10, 574–576, May 16, 2019.

4. Piao, D. and Y. Wang, "Tripolarized MIMO antenna using a compact single-layer microstrip patch," *IEEE Transactions on Antennas and Propagation*, Vol. 67, No. 3, March 2019.
5. Kumar, N. and U. K. Kommuri, "MIMO antenna mutual coupling reduction for WLAN using spiro meander line UC-EBG," *Progress In Electromagnetics Research C*, Vol. 80, 65–77, 2018.
6. Firmansyah, T., S. Praptodiyono, Herudin, D. Aribowo, S. Alam, D. WidiAstuti, and M. Yunus, "Bandwidth enhancement and miniaturization of circular-shaped microstrip antenna based on beleved half-cut structure for MIMO 2×2 application," *International Journal of Electrical and Computer Engineering*, Vol. 9, No. 2, 1110–1121, 2019.
7. Dkiouak A., M. El Ouahabi, A. Zakriti, M. Khalladi, and A. Mchbal, "Design of a compact hexagonal structured dual band MIMO antenna using orthogonal polarization for WLAN and satellite applications," *International Journal of Electrical and Computer Engineering*, Vol. 9, No. 5, 2019.
8. Hamid, A. K. and W. Obaid, "Hexa-band MIMO CPW bow-tie aperture antenna using particle swarm optimization," *International Journal of Electrical and Computer Engineering*, Vol. 8, No. 5, 2019.
9. Sekhar, M. and N. Suman, "CPW fed super-wideband antenna for microwave imaging application," *Progress In Electromagnetics Research C*, Vol. 130, 201–212, 2023.
10. Sura, P. R., M. Sekhar, and K. A. Kumar, "Design of dual-band notched UWB antenna loaded with split ring resonators for wide band rejection," *International Journal of Electronics Letters*, Vol. 11, 2023.
11. Sekhar, M. and S. Nelaturi, "Wideband circular polarized meandered patch antenna for microwave imaging," *Analog Integrated Circuits and Signal Processing*, Vol. 111, 81–88, 2022.
12. Sura, P. R., M. Sekhar, and A. K. Kumar, "Quad band printed antenna for Wi-Fi, WLAN, C-band and WiMAX applications," *Wireless Personal Communications*, Vol. 124, 437–448, 2022.
13. Sura, P. R. and M. Sekhar, "Circularly polarized dual band dual slot antenna for WLAN, Wi-MAX and Wi-Fi applications," *IETE Journal of Research*, Vol. 69, No. 3, 2023.
14. Hafezifard, R., M. Naser-Moghadasi, and J. Rashed Mohassel, "Mutual coupling reduction for two closely spaced meander line antennas using metamaterial substrate," *IEEE Antennas and Wireless Propagation Letters*, Vol. 15, 40–43, IEEE, 2016.
15. Farahani, M., M. Akbari, M. Nedil, and T. A. Denidni, "Mutual coupling reduction in dielectric resonator MIMO antenna arrays using metasurface orthogonalize wall," *2017 11th European Conference on Antennas and Propagation (EUCAP)*, 2017.
16. Farahani, M. and J. Pourahmadazar, "Mutual coupling reduction in millimeter-wave MIMO antenna array using a metamaterial polarization-rotator wall," *IEEE Antennas and Wireless Propagation Letters*, Vol. 16, 2324–2327, IEEE, 2016.
17. Tang, Z., X. Wu, J. Zhan, Z. Xi, and S. Hu, "A novel miniaturized antenna with multiple band-notched characteristics for UWB communication applications," Journal of Electromagnetic Waves and Applications, Vol. 32, No. 15, 1961–1972, 2018.
18. Zhao, X., S. P. Yeo, and L. C. Ong, "Planar UWB MIMO antenna with pattern diversity and isolation improvement for mobile platform based on the theory of characteristic modes," *IEEE Trans. Antennas Propag.*, Vol. 66, No. 1, 420–425, January 2018.
19. Khan, S. M., A. Iftikhar, S. M. Asif, A.-D. Capobianco, and B. D. Braaten, "A compact four elements UWB MIMO antenna with on-demand WLAN rejection," *Microw. Opt. Technol. Lett.*, Vol. 58, No. 2, 270–276, February 2016.
20. Biswal, S. P. and S. Das, "A low-profile dual port UWB-MIMO/diversity antenna with band rejection ability," *Int. J. RF. Microw. Comput.-Aided Eng.*, Vol. 28, No. 1, Art. No. e21159, January 2017.
21. Liu, Y.-Y. and Z.-H. Tu, 'Compact differential band-notched stepped-slot UWB-MIMO antenna with common-mode suppression," *IEEE Antennas Wireless Propag. Lett.*, Vol. 16, 593–595, 2017.

22. Ojaroudi Parchin, N., H. Jahanbakhsh Basherlou, Y. I. Al-Yasir, A. Ullah, R. A. Abd-Alhameed, and J. M. Noras, "Multi-band MIMO antenna design with user-impact investigation for 4G and 5G mobile terminals," *Sensors*, Vol. 19, 456, 2019.
23. Hussain, R., A. T. Alreshaid, S. K. Podilchak, and M. S. Sharawi, "Compact 4G MIMO antenna integrated with a 5G array for current and future mobile handsets," *IET Microw. Antennas Propag.*, Vol. 11, 271–279, 2017.
24. Chen, Q., H. Lin, J. Wang, L. Ge, Y. Li, and T. Pei, "Single ring slot-based antennas for metal-rimmed 4G/5G smartphones," *IEEE Trans. Antennas Propag.*, Vol. 67, 1476–1487, 2018.
25. Abdulkawi, W. M., W. A. Malik, S. U. Rehman, A. Aziz, A. F. A. Sheta, and M. A. Alkanhal, "Design of a compact dual-band MIMO antenna system with high-diversity gain performance in both frequency bands," *Micromachines*, Vol. 12, No. 4, 383, 2021.